Energy & Environmental Science

Varying the ionic functionalities of conjugated polyelectrolytes leads to both p- and n-type carbon nanotube composites for flexible thermoelectrics

Journal:	*Energy & Environmental Science*
Manuscript ID:	EE-COM-03-2015-000938.R1
Article Type:	Communication
Date Submitted by the Author:	22-Apr-2015

Complete List of Authors:	Bazan, Guillermo; University of California, Department of Chemistry Mai, Cheng; University of California, Russ, Boris; UC Berkeley, Chemical and Biomolecular Engineering; UC Berkeley, Dept of Chemical Engineering, Fronk, Stephanie; University of California, Hu, Nan; University of California, Chan-Park, Mary; Nanyang Technical University, Department of Mechanical Engineering Urban, Jeffrey; Lawrence Berkeley National Laboratory, Segalman, Rachel; University of California-Berkeley, Dept. of Chemical Engineering Chabinyc, Michael L. ; University of California, Santa Barbara, Materials Department

Table of Content Graphic:

Selective doping of single-walled carbon nanotubes can be achieved by varying pendant ionic functionalities of conjugated polyelectrolytes.

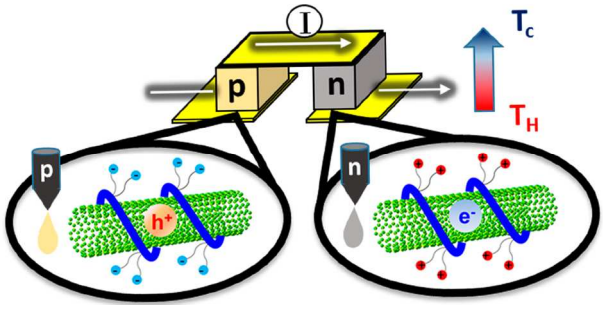

Energy & Environmental Science RSCPublishing

COMMUNICATION

Varying the ionic functionalities of conjugated polyelectrolytes leads to both *p*- and *n*-type carbon nanotube composites for flexible thermoelectrics

Cite this: DOI: 10.1039/xoxxoooooox

Received ooth January 2015,
Accepted ooth January 2015

DOI: 10.1039/xoxxoooooox

www.rsc.org/

Cheng-Kang Mai,[a] Boris Russ,[b] Stephanie L. Fronk,[a] Nan Hu,[a] Mary B. Chan-Park,[c] Jeffrey J. Urban,[b,d] Rachel A. Segalman,[e] Michael L. Chabinyc,[e] and Guillermo C. Bazan*[a,e]

Single-walled carbon nanotubes can be selectively doped by conjugated polyelectrolytes (CPEs) to form either *p*- or *n*-type composites. The selectivity of charge-transfer doping is found to be dictated by the polarities of CPE pendant ionic functionalities. This finding leads to a fundamentally new approach to both *p*- and *n*-type solution-processable composites for high performance, flexible thermoelectric devices.

Broader context

Thermoelectric devices that convert a heat gradient directly to electricity without any moving parts are considered as a clean technology for energy conversion. In order to fabricate a thermoelectric module, both hole-transporting (*p*-type) and electron-transporting (*n*-type) conductive materials are required. Polymer/carbon nanotube composites are relevant in this context due to their excellent electrical properties and the mechanical strength in thin films afforded by the carbon nanotubes. Conjugated polyelectrolytes (CPEs), a group of semiconducting polymers with pendant ionic functionalities, can serve as dispersants of carbon nanotube into environmentally friendly solvents, such as water. In this contribution, we show that CPEs work as efficient dopants for single-walled carbon nanotubes (SWNTs) and thereby can be used to provide either *p*-type or *n*-type solution-processable composites, depending on the choice of pendant ionic functionality. Taking into account these considerations allows us to fabricate high performance flexible thermoelectric modules by combination of suitable CPE/SWNT composites.

Single-walled carbon nanotubes (SWNTs) are attractive materials for developing flexible organic electronics,[1] given their outstanding chemical,[2] electrical,[3] and mechanical properties.[4] As synthesized SWNTs exist as bundles, due to the strong inter-tube interactions. To enable solution processing, a variety of conjugated polymers have been used as SWNT dispersants.[5] Conjugated polyelectrolytes (CPEs), namely conjugated polymers with pendant ionic functionalities, are particularly interesting.[6] They not only provide hydrophobic interactions between the conjugated backbones and the SWNT surfaces, but also render the CPE/SWNT complexes miscible in polar solvents due to the presence of ionic functionalities. The optical, mechanical, and electrical properties of these composites can be tailored without negatively impacting the desirable electronic properties of SWNTs. Such non-covalent composite systems when there is no covalent bond between the CPE and the SWNT, can therefore be preferable to counterparts that include modifications of SWNTs via chemical reactions.[7]

SWNT composites have found a variety of useful applications, such as optical probes for bioanalytical sensors,[8] organic solar cells,[9] field-effect transistors (FETs),[10] and thermoelectrics.[11] Pristine SWNTs frequently exhibit *p*-type charge transport behavior, due to hole generation upon oxidation by air, and most SWNT composites are typically *p*-type materials.[12] However, both *p*-type and *n*-type materials are desired for many organic electronics, such as thermoelectric module,[13] and field-effect transistors.[14] SWNTs can be intentionally *n*-type doped via reduction with potassium,[15] but the stability of the resulting materials may be insufficient for long term device applications. Metal-encapsulated carbon nanotubes,[16] and non-covalent functionalization of SWNTs with polymers[10a,11e-j] or electron-rich small molecules[11k] also provides *n*-type SWNT composites, which are usually processed as buckypapers via filtration. While CPEs have been shown to aid the solution-processability of SWNTs, their use as charge-transfer dopants for SWNTs has not been reported.[5b]

Herein, we report the selective doping of SWNTs by CPEs to provide either *p*- or *n*-type composites, via a process that is dictated by the choice of ionic functional group. Specifically, it is possible to use anionic and cationic CPEs with the same conjugated backbone to

provide *p*-type and *n*-type conductive composites, respectively. Furthermore, we utilize both the hole and electron transporting CPE/SWNT composites to successfully demonstrate an efficient flexible thermoelectric device.

Fig. 1 provides the molecular structures of the four CPEs included in our studies. Detailed synthetic procedures and characterization are provided in the Supporting Information (SI).[17] PFBT-Na and PFBT-PyrBIm$_4$ share the same conjugated backbone, poly(fluorene-*alt*-benzothiadiazole) (PFBT), but contain tethered anionic (sulfonates) and cationic (pyridinium) groups, respectively. Similarly, CPE-Na and CPE-PyrBIm$_4$ possess the narrow bandgap conjugated backbone, poly(cyclopenta-[2,1-b;3,4-b']-dithiophene-*alt*-4,7-(2,1,3-benzothiadiazole)) (CPDT-*alt*-BT), but contain different ionic groups. These four polymers allow us a unique opportunity to untangle the influence of the conjugated backbone and the pendant ionic functionalities on electronic properties.

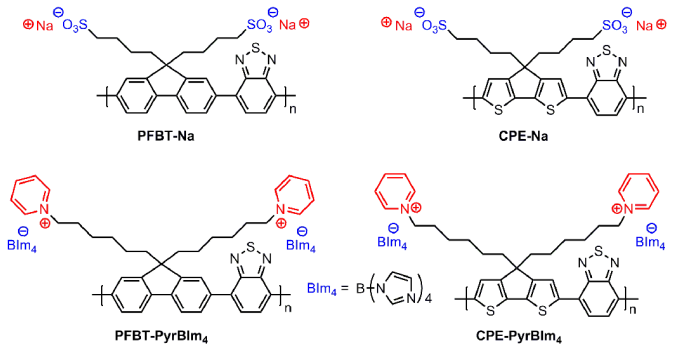

Fig. 1 Chemical structures of CPEs studied. Pendant ionic functionalities and counterions are colored, negative charged ones are blue and positive charged ones are red.

The CPE/SWNT composite films were characterized by measurements under nitrogen of electrical conductivity (σ) and *Seebeck* coefficient (S). Standard four point probe measurements were used to measure σ. As described in more detail in the SI, S was determined by linear fitting of data taken by imposing temperature differences across the sample and measuring the corresponding thermovoltages ($S = -\Delta V/\Delta T$). The selectivity of the doping is verified by the sign of the S values, of which positive and negative signs indicate *p*- and *n*-type charge transport, respectively.[13] Power factors ($PF = \sigma S^2$) were calculated accordingly.

We first compare the influence of the conjugated backbone (PFBT-Na vs. CPE-Na) on the properties of anionic CPE/SWNT composites. It is worth noting that CPE-Na is readily doped during dialysis in water leading to conductive films,[17b,18] while PFBT-Na remains neutral and thus leads to relatively insulating films due to the low density of free charge carriers. We therefore expected to observe different electrical behavior for these blends using polymers with the same ionic side chains and counterions, but different conjugated backbones.

The electrical conductivity and relevant thermoelectric properties of PFBT-Na/SWNT composites at different weight ratios are shown in Fig. 2a. One observes that σ increases progressively as the SWNT loading increases. S remains positive, which is indicative of *p*-type conduction, and is not affected by the range of loadings examined in these studies. The PF values therefore increase because of the increase in σ. In homogeneous semiconductors one typically finds an inverse relationship of σ and S, due to the increase in carrier concentration with larger electrical conductivity.[13] However, in heterogeneous materials, such as composites, this relationship does not necessarily hold due to the percolation of charge carriers through the two materials and across interfaces.[19] The insensitivity of S in these blends to different loadings and the similarity of the values (~65 μV/K) to that observed in SWNT-only sample (62 μV/K, see Table 2, entry 5)[11] suggests that the SWNTs dominate S in the PFBT-Na/SWNT blends.

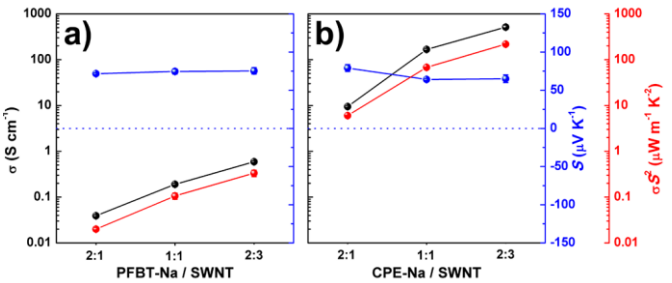

Fig. 2 Electrical conductivity (σ, black); *Seebeck* coefficient (S, blue); and power factor ($PF = \sigma S^2$, red) as a function of different weight ratios for: a) PFBT-Na/SWNT and b) CPE-Na/SWNT. [CPE] = 2 mg mL^{-1} is constant in all dispersions. Note that σ and PF are plotted on a log scale, while S is plotted on a linear scale.

A different behavior is observed with CPE-Na/SWNT blends (Fig. 2b). As discussed above, CPE-Na is *p*-doped in solution, and therefore, one can measure σ (0.16 ± 0.005 S cm^{-1}) and S (165 ± 25 μV K^{-1}) for neat CPE-Na films.[20] Incorporation of SWNTs at the lowest ratio in our studies, *i.e.* CPE-Na/SWNT = 2:1 by weight, yields an approximately 60-fold increase in σ. The value of σ continues to increase as the SWNT content increases, and reaches 514 ± 55 S cm^{-1} at the 2:3 weight ratio. Similar to the case of PFBT-Na/SWNT composites, S remains largely unchanged. The similar values to the PFBT-Na/SWNT blends, where the polymer is undoped, suggest that S is again dominated by the SWNTs. The doped nature of CPE-Na likely increases the electrical conductivity by reducing the inter-SWNT contact resistance. The higher σ of CPE-Na/SWNT composites, relative to PFBT-Na/SWNT, leads to a larger PF, reaching up to 218 ± 89 μW m^{-1} K^{-2} at the 2:3 weight ratio. This is the highest PF value obtained in all of the CPE/SWNT blends examined in our studies. It should be noted that efforts to increase [SWNT] in the parent dispersions led to high viscosity, which prevented processing of the composites.

Scanning electron microscopy (SEM) images of CPE-Na/SWNT films deposited on silicon substrates as a function of composition are provided in Fig. 3. These data show that the composite films are heterogeneous, and that they become more densely packed at higher loadings leading to a large number of inter-SWNT contacts. Also provided in Fig. 3d is the image of a much thicker film that was prepared by drop-casting from 2:3 weight ratio of CPE-Na/SWNT in MeOH/water (1:1 vol:vol). One can therefore tune the thickness of the active layer depending on the desired applications.

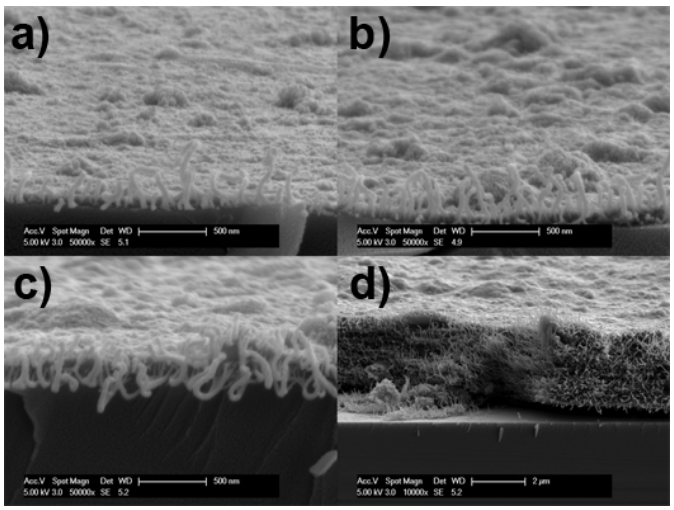

Fig. 3 Scanning electron microscopy (SEM) images of CPE-Na/SWNT films (cross-section) at different weight ratio on silicon, a) 2:1 (spin-coating); b) 1:1 (spin-coating); c) 2:3 (spin-coating); and d) 2:3 (drop-casting).

Surprisingly, we find that the charge carrier type in the blends can be switched by changing the side chains and counterions in the CPE structure. The electronic characteristics of PFBT-PyrBIm$_4$/SWNT and CPE-PyrBIm$_4$/SWNT, which have cationic side chains, are very different from their anionic counterparts (Fig. 4). Our analysis begins by examinations of *S*. At low SWNT content, the negative *S* values measured for PFBT-PyrBIm$_4$/SWNT (–21 ± 3 μV K^{-1} at 2:1 weight ratio) and CPE-PyrBIm$_4$/SWNT (–55 ± 8 μV K^{-1} at 2:1) indicate that the predominant charge carriers in the composites are electrons. Therefore, these cationic CPEs behave like *n*-type dopants.[21] CPE-PyrBIm$_4$ appears to be a more persistent *n*-type dopant, because the composite retains the negative coefficient at 1:1 content (–41 ± 6 μV K^{-1}). At the highest SWNT content (2:3 CPE/SWNT weight ratio), both CPE-PyrBIm$_4$ (52 ± 8 μV K^{-1}) and PFBT-PyrBIm$_4$ (31 ± 5 μV K^{-1}) composites regain the *p*-type transport, which is characteristic of the carbon nanotubes themselves. These observations thus reveal the ability to tune the predominant charge carrier in the composite via the ratio of the components.

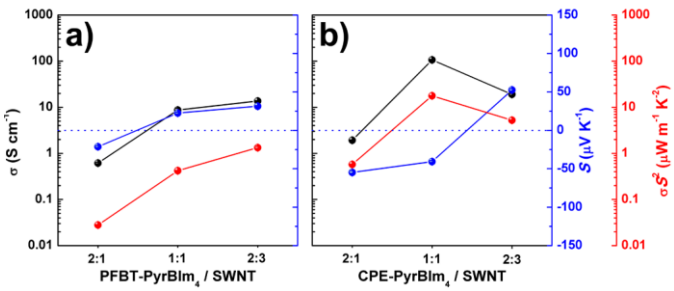

Fig. 4 Electrical conductivity (σ, black); *Seebeck* coefficient (*S*, blue); and power factor (*PF* = σ*S*^{2}, red) as a function of different weight ratios for: a) PFBT-PyrBIm$_4$/SWNT and b) CPE-PyrBIm$_4$/SWNT. [CPE] = 2 mg mL^{-1} is constant in all dispersions. Note that σ and *PF* are plotted on a log scale, while *S* is plotted on a linear scale.

Fig. 4 also reveals a complex behavior for σ in the cationic CPE/SWNT films, particularly for CPE-PyrBIm$_4$/SWNT, for which a maximum is observed in the 1:1 blend. Our working hypothesis is that CPE-PyrBIm$_4$ can *n*-dope the nanotubes and a higher *n*-type charge carrier density is therefore achieved when the SWNT content is lower. The SWNTs will still likely provide the dominant contribution to σ due to their higher charge mobility. *S* is a weighted average of the contributions of holes and electrons, and it is possible that the relatively lower values of *S* in these blends vs. those of PFBT-Na and CPE-Na (~ 65 μV K^{-1}) are due to the competition between *p*- and *n*-type conductions. As the amount of SWNTs increases, one observes a shift to overall *p*-type transport in the 2:3 system. These observations suggest that the conventional *p*-doping of the SWNT is no longer compensated by *n*-type doping by the cationic CPEs. Under these scenarios, less efficient doping by CPE-PyrBIm$_4$ in the 2:3 composite possibly results in a lower effective charge carrier density, thus leading to a lower σ (19 ± 1 S cm^{-1}). Therefore, the highest *PF* we obtained for *n*-type CPE-PyrBIm$_4$/SWNT composite is 17.8 ± 5.8 μW m^{-1} K^{-2} in the 1:1 blend.

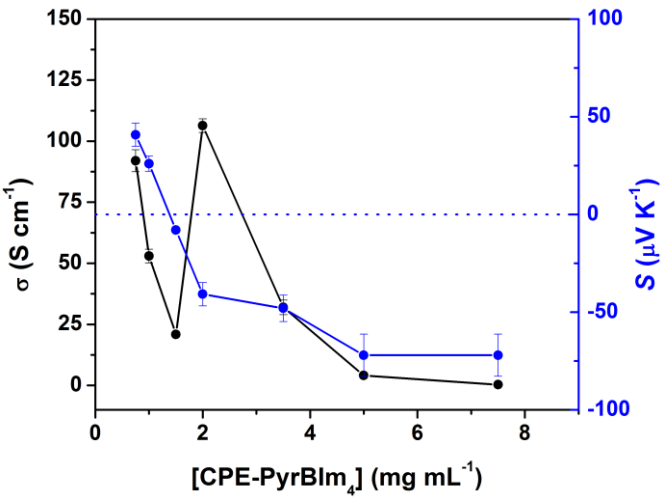

Fig. 5 Thermoelectric properties of CPE-PyrBIm$_4$/SWNT composite spin-coated films ([SWNT] = 2 mg/mL) as a function of CPE-PyrBIm$_4$ concentration in dispersions. Plotted values correspond to the average of three independent measurements.

That CPE-PyrBIm$_4$ is an *n*-type dopant for SWNTs is substantiated by examination of composites prepared from dispersions with constant [SWNT] = 2 mg mL^{-1} and varying [CPE-PyrBIm$_4$]. Fig. 5 shows the change of σ and *S* as a function of [CPE-PyrBIm$_4$]. As [CPE-PyrBIm$_4$] increases, *S* gradually decreases, turns into negative values, and finally stabilizes at –78 ± 10 μV K^{-1}. The interpretation of σ is nontrivial. When [CPE-PyrBIm$_4$] = 0.75 mg mL^{-1}, σ = 92 ± 6 S cm^{-1}, which is the highest σ of *p*-type composites. As [CPE-PyrBIm$_4$] increases, the hole concentration in the composites decreases, and results in a local minimum of σ at [CPE-PyrBIm$_4$] = 1.5 mg mL^{-1}, at which point, the absolute value of *S* is also the minimum. Further increase of [CPE-PyrBIm$_4$] leads to *n*-type composites, and a maximum σ is observed at [CPE-PyrBIm$_4$] =

2 mg mL^{-1}. Similar behaviors are also observed in *n*-type SWNT composites with molecular dopants,[11k] and this can explain why higher [SWNT] provides a lower σ in the CPE-$PyrBIm_4$/SWNT (2:3) system in Fig. 4b, because of the switch of the predominant charger carriers. However, overloading of CPE-$PyrBIm_4$ will dilute inter-SWNT contacts to provide less conducting materials with stable negative *S* at –72 μV K^{-1}. Overall, this study indicates that a careful tuning of the amount of *n*-type dopants is required in order to obtain SWNT composites with high σ while retaining the negative *S*.

Examination of the ionization energies (IE) and electron affinities (EA) of the CPEs provides a basis to understand the charge-transfer doping of SWNTs (Table 1). IEs were obtained by ultraviolet photoelectron spectroscopy (UPS) measurement, while EAs were estimated by subtracting the optical bandgap from the IE. Interestingly, for PFBT-Na (IE = 5.4 eV, |EA| = 3.0 eV) and PFBT-$PyrBIm_4$ (IE = 5.5 eV, |EA| = 3.2 eV) with the same conjugated backbones, pendant ionic functionalities do not change the IE and EA significantly. The narrow bandgap cationic CPE-$PyrBIm_4$ (IE = 4.7 eV, |EA| = 3.3 eV) displays a similar EA, but a lower IE due to the electron-rich CPDT monomer units. It is known from the literature that molecular dopants with |EA| > 2.7 can behave as *p*-type dopants for SWNTs, while molecules with IE < 5.6 eV can *n*-dope effectively.[11k] Under this scenario, PFBT-Na, PFBT-$PyrBIm_4$ and CPE-$PyrBIm_4$ have the potential to serve as either *p*-type or *n*-type dopants for SWNTs. The pendant charged groups of CPEs enable functionality beyond providing the solubility in polar media. Note also that CPE-Na is not included in these considerations because it is intrinsically doped.

A series of control experiments were conducted to further understand the *n*-type doping capability of CPEs with -$PyrBIm_4$ functionality. First, we would like to point out that PFBT-$PyrBIm_4$ is synthesized via a two-step sequence (see SI, Scheme S1). A CPE analogue PFBT-PyrBr with Br^- counterions is the precursor to PFBT-$PyrBIm_4$. With PFBT-PyrBr in hand, both σ and *S* of composite PFBT-PyrBr/SWNT at different weight ratios were measured (Table 2, entries 1, 3 and 4). Negative *S* was observed only at high [PFBT-PyrBr] (entry 4), at which point, σ (0.0076 S cm^{-1}) is too low to be useful for thermoelectric application. Considering the structural difference between PFBT-PyrBr and PFBT-$PyrBIm_4$ (Fig. 4a), the Pyr^+-BIm_4^- ion pair seems to be a more potent element to contribute to *n*-type SWNT doping.

Table 1 Ionization energy (IE) and electron affinity (EA) determined for the CPEs in this study.

CPE	IE (eV)[a]	|EA| (eV)[b]	Optical Bandgap (eV)[c]
PFBT-Na	–5.4	3.0	2.44
PFBT-$PyrBIm_4$	–5.5	3.2	2.32
CPE-$PyrBIm_4$	–4.7	3.3	1.38

[a] Obtained from UPS measurements; [b] Estimated by subtracting the optical bandgap from the |IE|; [c] Estimated from the onset of thin film absorption.

One possible hypothesis to consider is that the BIm_4^- ion could be an effective dopant. However, a control experiment of SWNT with $NaBIm_4$ (1:1 by weight, see SI, Fig. S7 for XPS analysis) does not show any significant change in either σ or *S* (Table 2, entries 5 and 6). BIm_4^- on its own is not an apparent *n*-type dopant for SWNTs.

Table 2 Thermoelectric properties (σ and *S*) of PFBT-PyrBr/SWNT composites and SWNT mats.

	Materials	σ (S cm^{-1})	*S* (μV K^{-1})	σS^2 (μW m^{-1} K^{-2})
1[a]	**PFBT-PyrBr/SWNT (2:1)**	0.80 ±0.04	78 ±12	0.49 ±0.17
2[a]	**PFBT-PyrBr/SWNT/$NaBIm_4$ (2:1:1)**	2.4 ±0.1	–13 ±2	0.041 ±0.014
3[a]	**PFBT-PyrBr/SWNT (3:1)**	0.020 ±0.001	78 ±12	0.012 ±0.004
4[a]	**PFBT-PyrBr/SWNT (5:1)**	0.0076 ±0.0004	–113 ±17	0.0097 ±0.0034
5[b]	**SWNT**	18.5 ±0.9	62 ±9	7.1 ±2.5
6[b]	**SWNT/$NaBIm_4$ (1:1)**	21.0 ±1.0	59 ±9	7.3 ±2.6

[a] [PFBT-PyrBr] = 2 mg mL^{-1} in all dispersions. [b] SWNT mats (~ 20 μm thick) were prepared by filtration of SWNT dispersion in H_2O:MeOH (1:1) on top of filter papers (cellulose acetate, pore size = 0.45 μm).

Another factor to consider is that the dipole of the Pyr^+-BIm_4^- ion pair facilitates the electron transfer from CPE to SWNT. Compared to the Br^- ion, BIm_4^-, known as a bulky, non-coordinating counterion, has a longer distance from the Pyr^+ cation, thus forming a larger dipole moment. This large dipole may be accounted for the *n*-type SWNT doping. Interestingly, adding $NaBIm_4$ to PFBT-PyrBr/SWNT (2:1) dispersion converts the original *p*-type composite into *n*-type, concomitant with the formation of the Pyr^+-BIm_4^- ion pair. These observations highlight that the chemical nature of the ion pair is essential for determining the dopant strength. However, we lack structural insight into the exact spatial organization (i.e. distance between the CPE backbone and SWNT surface, orientation/location of the electrostatic dipoles) to provide a detailed account of the forces of interactions that come together for favoring one type of charge carrier relative to the other.

The selective doping in CPE/SWNT composites provides a path to access both *p*- and *n*-type conductive materials for

thermoelectric applications. A flexible, radial thermoelectric module was thus fabricated using CPE-Na/SWNT (1:1) as *p*-legs and CPE-PyrBIm$_4$/SWNT (1:1) as *n*-legs (Fig. 6) on a Kapton® (polyimide) substrate. The CPE/SWNT composites were simply drop-cast and dried on the flexible substrates, compared to the fabrication of buckypapers via filtration as in the previous reports.[11,16b] This module can be used to harness thermal gradients in customizable geometries. Successful operation of a radial module configuration surrounding a localized hot spot was confirmed by the additive character of the open-circuit voltages (V_{oc}) as more *p*- and *n*-legs are added in series to assemble the module (Fig. 6e), and the successfully generated power under a temperature bias (Fig. 6f). These power outputs are comparable to values reported for small molecule doped SWNTs when accounting for the differences in thicknesses of the *p*- and *n*-legs used in the respective modules.[11k] The module shows no deterioration on the performance after at least 200 working cycles near room temperature (see SI, Fig. S8), and it can function successfully with the hot side temperature up to 100 °C.

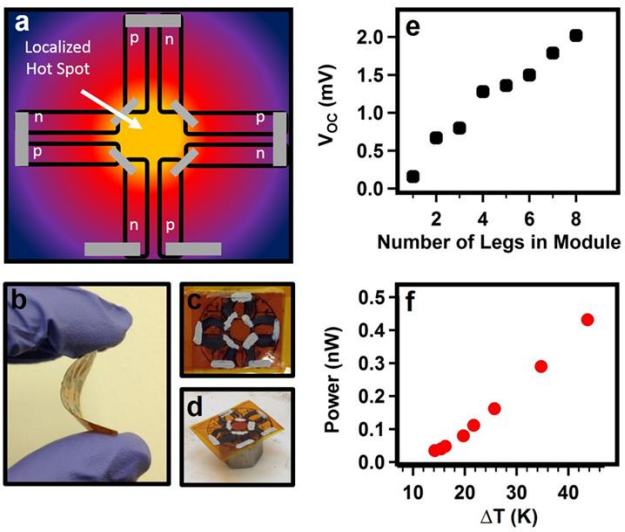

Fig. 6 Radial thermoelectric generator. a) Schematic of a planar module configuration which can be utilized to harness radial thermal gradients generated from a localized hot spot; b) Deposition on a Kapton substrate enables module flexibility; c) A thermoelectric generator is constructed using CPE-Na/SWNT (1:1) as *p*-legs and CPE-PyrBIm$_4$ (1:1) as *n*-legs. Metal contacts are shown in grey; d) A flat tipped, metal heating block provided the localized heating; e) Open-circuit voltage (V_{oc}) increases as more *p*- and *n*-legs are added in series to assemble the module under a temperature gradient (ΔT = 10K as determined using an infra-red camera); f) Power generation by the 8-leg module shown in c) under varied temperature gradients.

Conclusions

To summarize, we have demonstrated the selective charge-transfer doping of SWNTs by using CPEs with identical conjugated backbone but different pendant ionic functionalities. Specifically, CPEs with anionic or cationic side chains provide *p*-type or *n*-type conductive CPE/SWNT composites, respectively, at non-excess loadings of SWNTs. We find that using the self-doped[22] CPE-Na as the dispersing agent leads to composites with relatively high conductivity, because of the minimization of inter-SWNT contact resistance in the composite. Remarkably, the cationic CPE/SWNT composites exhibit negative *S*, indicative of *n*-type doping of SWNT. Due to the synthetic versatility of cationic CPEs, our studies provide a new strategy to obtain *n*-type SWNT composites. Both *p*- and *n*-type CPE/SWNT composites have been used to fabricate an efficient flexible thermoelectric module. Importantly, these CPE/SWNT composites are capable of solution-processing from aqueous mixtures, such as spin-coating, drop-casting, and possibly inject-printing, all of which are highly desired for the future printed flexible electronics.

Notes and references

[a] Center for Polymers and Organic Solids, Department of Chemistry and Biochemistry, University of California, Santa Barbara, CA 93106, USA
E-mail: bazan@chem.ucsb.edu
[b] Department of Chemical and Biomolecular Engineering, UC Berkeley, Berkeley, CA 94720
[c] School of Chemical and Biomedical Engineering, Nanyang Technological University, 62 Nanyang Drive, 637459, Singapore
[d] The Molecular Foundry, Materials Sciences Division, Lawrence Berkeley National Lab, Berkeley, CA 94720, USA
[e] Materials Department, Materials Research Laboratory
University of California, Santa Barbara, CA 93106, USA

† Electronic Supplementary Information (ESI) available: [detailed synthesis and characterization of polymers, processing and thermoelectric measurements, fabrication and characterization of thermoelectric module]. See DOI: 10.1039/c000000x/

Acknowledgements

We acknowledge financial support from the AFOSR MURI FA9550-12-1-0002. The MRL Shared Experimental Facilities (SEM, UPS, and GPC) are supported by the MRSEC Program of the NSF under Award No. DMR 1121053; a member of the NSF-funded Materials Research Facilities Network (www.mrfn.org). Portions of this research were carried out at the Molecular Foundry, a Lawrence Berkeley National Laboratory user facility supported by the Office of Science, Office of Basic Energy Sciences, U.S. Department of Energy, under Contract DE-AC02-05CH11231. C.-K. Mai thanks Prof. Thuc-Quyen Nguyen and Dr. Xiaofeng Liu for helpful discussions, Dr. Ruth Schlitz and Anne Glaudell for help on thermoelectric measurements.

References

1 a) C. Wang, K. Takei, T. Takahashi and A. Javey, *Chem. Soc. Rev.*, 2013, **42**, 2592; b) Park, S.; Vosguerichian, M. and Bao, Z. *Nanoscale*, 2013, **5**, 1727.

2 S. Niyogi, M. A. Hamon, H. Hu, B. Zhao, P. Bhowmik, R. Sen, M. E. Itkis and R. C. Haddon, *Acc. Chem. Res.*, 2002, **35**, 1105.

3 a) H. Dai, E. W. Wong and C. M. Lieber, *Science*, 1996, **272**, 523; b) S. Tans, M. Devoret, H. Dai and A. Thess, *Nature*, 1997, **386**, 474; c) K. S. Novoselov, A. K. Geim, S. V. Morozov, D. Jiang, Y. Zhang, S. V. Dubonos, I. V. Grigorieva and A. A. Firsov, *Science*, 2004, **306**, 666.

4 M. M. J. Treacy, T. W. Ebbesen and J. M. Gibson, *Nature*, 1996, **381**, 678; b) M. D. Lima, N. Li, M. J. de Andrade, S. Fang, S. J. Oh, G. M. Spinks, M. E. Kozlov, C. S. Haines, D. Suh, J. Foroughi, S. J. Kim, Y. Chen, T. Ware, M. K. Shin, L. D. Machado, A. F. Fonseca, J. D. W. Madden, W. E. Voit, D. S. Galvão and R. H. Baughman, *Science*, 2012, **338**, 928.

5 S. K. Samanta, M. Fritsch, U. Scherf, W. Gomulya, S. Z. Bisri and M. A. Loi, *Acc. Chem. Res.*, 2014, **47**, 2446.

6 a) P. Deria, J.-H. Olivier, J. Park and M. J. Therien, *J. Am. Chem. Soc.*, 2014, **136**, 14193; b) Y. Li, C.-K. Mai, H. Phan, X. Liu, T.-Q. Nguyen, G. C. Bazan and M. B. Chan-Park, *Adv. Mater.*, 2014, **26**, 4697; c) P. Deria, C. D. V. Bargen, J.-H. Olivier, A. S. Kumbhar, J. G. Saven and M. J. Therien, *J. Am. Chem. Soc.*, 2013, **135**, 16220; d) T. Casagrande, P. Imin, F. Cheng, G. A. Botton, I. Zhitomirsky and A. Adronov, *Chem. Mater.*, 2010, **22**, 2741; e) F. Cheng, P. Imin, S. Lazar, G. A. Botton, G. de Silveira, O. Marinov, J. Deen and A. Adronov, *Macromolecules*, 2008, **41**, 9869

7 a) V. Sgobba and D. M. Guldi, *Chem. Soc. Rev.*, 2009, **38**, 165; b) P. Singh, S. Campidelli, S. Giordani, D. Bonifazi, A. Bianco and M. Prato, *Chem. Soc. Rev.*, 2009, **38**, 2214.

8 a) D. A. Heller, S. Baik, T. E. Eurell and M. S. Strano, *Adv. Mater.*, 2005, **17**, 2793; b) D. A. Heller, H. Jin, B. M. Martinez, D. Patel, B. M. Miller, T.-K. Yeung, P. V Jena, C. Höbartner, T. Ha, S. K. Silverman and M. S. Strano, *Nat. Nanotechnol.*, 2009, **4**, 114; c) Y. Liu, J. Huang, M.-J. Sun, J.-C. Yu, Y.-L. Chen, Y.-Q. Zhang, S.-J. Jiang and Q.-D. Shen, *Nanoscale*, 2014, **6**, 1480; d) J. Budhathoki-Uprety, P. V Jena, D. Roxbury and D. A. Heller, *J. Am. Chem. Soc.*, 2014, **136**, 15545.

9 a) S. Cataldo, P. Salice, E. Menna and B. Pignataro, *Energy Environ. Sci.*, 2012, **5**, 5940; b) D. D. Tune and J. G. Shapter, *Energy Environ. Sci.*, 2013, **6**, 2572; c) L. Wang, H. Liu, R. M. Konik, J. A. Misewich and S. S. Wong, *Chem. Soc. Rev.*, 2013, **42**, 8134.

10 a) M. Shim, A. Javey, N. W. S. Kam and H. Dai, *J. Am. Chem. Soc.*, 2001, **123**, 11512; b) A. Javey, R. Tu, D. B. Farmer, J. Guo, R. G. Gordon and H. Dai, *Nano Lett.*, 2005, **5**, 345; c) J. Li, Y. Huang, P. Chen and M. B. Chan-Park, *Chem. Mater.*, 2013, **25**, 4464.

11 Review: a) C. A. Hewitt and D. L. Carroll, *Polymer Composites for Energy Harvesting, Conversion, and Storage*, Ch. 9, 191–211, ACS Symposium Series, Vol. 1161, 2014; For selected examples: b) D. Kim, Y. Kim, K. Choi, J. C. Grunlan and C. Yu, *ACS Nano*, 2010, **4**, 513; c) Q. Yao, L. Chen, W. Zhang, S. Liufu and X. Chen, *ACS Nano*, 2010, **4**, 2445; d) W. Zhao, S. Fan, N. Xiao, D. Liu, Y. Y. Tay, C. Yu, D. Sim, H. H. Hng, Q. Zhang, F. Boey, J. Ma, X. Zhao, H. Zhang and Q. Yan, *Energy Environ. Sci.*, 2012, **5**, 5364; e) C. Yu, K, Choi, L. Yin and J. C. Grunlan, *ACS Nano*, 2011, **5**, 7885; f) J. Liu, J. Sun, and L. Gao, *Nanoscale*, 2011, **3**, 3616; g) C. Yu, A. Murali, K. Choi and Y. Ryu, *Energy Environ. Sci.*, 2012, **5**, 9481; h) D. D. Freeman, K. Choi and C. Yu, *PLoS One*, 2012, **7**, e47822; i) G. P. Moriarty, J. N. Wheeler, C. Yu and J. C. Grunlan, *Carbon*, 2012, **50**, 885; j) G. P. Moriarty, K. Briggs, B. Stevens, C. Yu and J. C. Grunlan, *Energy Technol.*, 2013, **1**, 265; k) Y. Nonoguchi, K. Ohashi, R. Kanazawa, K. Ashiba, K. Hata, T. Nakagawa, C. Adachi, T. Tanase and T. Kawai, *Sci. Rep.*, 2013, **3**, 3344.

12 a) J. Kong, N. R. Franklin, C. Zhou, M. G. Chapline, S. Peng, K. Cho and H. Dai, *Science*, 2000, **287**, 622; b) P. G. Collins, *Science*, 2000, **287**, 1801; c) K. Bradley, S. Jhi, P. Collins, J. Hone, M. Cohen, S. Louie and A. Zettl, *Phys. Rev. Lett.*, 2000, **85**, 4361.

13 Reviews: a) Y. Chen, Y. Zhao and Z. Liang, *Energy Environ. Sci.*, 2015, **8**, 401; b) B. T. McGrail, A. Sehirlioglu and E. Pentzer, *Angew. Chem., Int. Ed.*, 2015, **2**, 1710; c) Q. Zhang, Y. Sun, W. Xu and D. Zhu, *Adv. Mater.*, 2014, **26**, 6829; d) M. Culebras, C. Gómez and A. Cantarero, *Materials*, 2014, **7**, 6701; e) M. He, F. Qiu and Z. Lin, *Energy Environ. Sci.*, 2013, **6**, 1352; f) O. Bubnova and X. Crispin, *Energy Environ. Sci.*, 2012, **5**, 9345; g) T. O. Poehler and H. E. Katz, *Energy Environ. Sci.*, 2012, **5**, 8110; h) N. Dubey and M. Leclerc, *J. Polym. Sci. Part B Polym. Phys.*, 2011, **49**, 467.

14 Reviews: a) J. E. Anthony, A. Facchetti, M. Heeney, S. R. Marder and X. Zhan, *Adv. Mater.*, 2010, **22**, 3876; b) Q. Meng and W. Hu, *Phys. Chem. Chem. Phys.*, 2012, **14**, 14152; c) Y. Zhao, Y. Guo, Y. Liu, *Adv. Mater.*, 2013, **25**, 5372; d) X. Gao and Y. Hu, *J. Mater. Chem. C*, 2014, **2**, 3099.

15 R. S. Lee, H. J. Kim, J. E. Fischer and A. Thess, *Nature*, 1997, **388**, 255.

16 a) T. Takenobu, T. Takano, M. Shiraishi, Y. Murakami, M. Ata, H. Kataura, Y. Achiba and Y. Iwasa, *Nat. Mater.*, 2003, **2**, 683; b) T. Fukumaru, T. Fujigaya, N. Nakashima, *Sci. Rep.*, 2015, **5**, 7951.

17 a) Z. B. Henson, Y. Zhang, T.-Q. Nguyen, J. H. Seo and G. C. Bazan, *J. Am. Chem. Soc.*, 2013, **135**, 4163; b) C.-K. Mai, H. Zhou, Y. Zhang, Z. B. Henson, T.-Q. Nguyen, A. J. Heeger and G. C. Bazan, *Angew. Chem. Int. Ed.*, 2013, **52**, 12874.

18 a) H. Zhou, Y. Zhang, C.-K. Mai, S. D. Collins, T.-Q. Nguyen, G. C. Bazan and A. J. Heeger, *Adv. Mater.*, 2014, **26**, 780; b) H. Zhou, Y. Zhang, C.-K. Mai, J. Seifter, T.-Q. Nguyen, G. C. Bazan and A. J. Heeger, *ACS Nano*, 2015, **9**, 371; c) H. Zhou, Y. Zhang, C.-K. Mai, S. D. Collins, G. C. Bazan, T.-Q. Nguyen and A. J. Heeger, *Adv. Mater.*, 2015, **27**, 1767.

19 A. M. Glaudell, J. E. Cochran, S. N. Patel and M. L. Chabinyc, *Adv. Energy Mater.*, 2015, **5**, 1401072.

20 C.-K. Mai, R. A. Schlitz, G. M. Su, D. Spitzer, X. Wang, S. L. Fronk, D.G. Cahill, M. L. Chabinyc and G. C. Bazan, *J. Am. Soc. Chem.*, 2014, **136**, 13478.

21 a) B. Russ, M. J. Robb, F. G. Brunetti, P. L. Miller, E. E. Perry, S. N. Patel, V. Ho, W. B. Chang, J. J. Urban, M. L. Chabinyc, C. J. Hawker and R. A. Segalman, *Adv. Mater.*, 2014, **26**, 3473; b) R. A. Schlitz, F. G. Brunetti, A. M. Glaudell, P. L. Miller, M. A. Brady, C. J. Takacs, C. J. Hawker and M. L. Chabinyc, M. L. *Adv. Mater.*, 2014, **26**, 2825.

22 M. S. Freund and B. A. Deore, *Self-Doped Conducting Polymers*, Wiley, Chichester, 2007.

Table of Content Graphic:

Selective doping of single-walled carbon nanotubes can be achieved by varying pendant ionic functionalities of conjugated polyelectrolytes.